Mater. Res. Soc. Symp. Proc. Vol. 958 © 2007 Materials Research Society 0958-L02-01

Silicon Photonic Devices and Polarisation Independence

Graham T. Reed, Goran Z. Mashanovich, Branislav D. Timotijevic, Frederic Y. Gardes, William R. Headley, and Nicholas Wright
Advanced Technology Institute, University of Surrey, Guildford, GU2 7XH, United Kingdom

ABSTRACT

Silicon Photonics is experiencing a dramatic increase in interest due to emerging application areas and several high profile successes in device and technology development. For both performance and cost reasons, there is a worldwide trend towards miniaturising silicon photonic waveguides. The shrinking of the device dimensions provides advantages in terms of cost and packing density, modulation bandwidth, improved performance in resonant structures, and an increase in optical power density within the devices. However, the size reduction comes at some costs in increased difficulty in maintaining single mode operation of the waveguides whilst controlling the polarisation properties of the device.

For some applications, it is essential that optical modulators and filters, as well as other components, operate in the single mode regime. It is also desirable that these components are polarisation insensitive. Design of the waveguide, which is the basic element of these devices, is therefore crucial. Due to the compatibility with single mode fibre dimensions as well as the possibility of control of polarisation, rib waveguides represent promising candidates for integration in SOI. The main limitation for rib waveguides is that the bend radius cannot always be sufficiently small to minimise the device footprint. Strip waveguides, on the other hand, are often considered as a good choice in this respect, as they allow very small bend radii resulting in a compact footprint. However, polarisation dependence of these waveguides can be significant. Therefore, both waveguide configurations are investigated in this paper, together with the implications for optical modulators.

Following from this discussion, we also consider optical modulators that operate in the depletion mode with the intrinsic bandwidth of several tens of gigahertz. We have previously reported a modulator based on a small rib waveguide with the height of < 500nm for high speed operation. However, in this paper we consider slightly larger designs to accommodate polarisation independence. Finally we discuss the characteristics of ring and racetrack resonators based on both rib and strip waveguides and methods of improving free spectral range whilst considering polarization effects. Both theoretical and experimental results are presented. The maximum free spectral range that we have demonstrated experimentally is ~43nm.

INTRODUCTION

Silicon Photonics is experiencing a dramatic increase in interest, due in part to recent demonstrations of fast modulators and devices of small footprint, occupying little valuable real estate. However, as device dimensions are reduced it becomes more difficult to equalise the device response to different polarisations of the input light wave. Should the device be fed by a fibre, this becomes particularly important because light from an optical fibre is typically of

random polarisation. In this paper we consider the implications of the desire for polarisation independence, as well as offering several device designs for comparative purposes.

WAVEGUIDE DESIGN

The fundamental building block of a photonic circuit is the optical waveguide itself. Modal and polarisation properties are two main concerns for the waveguide design. Waveguides that support more than a single mode are undesirable for optical communications as they may cause interference and, therefore result in degradation of device performance. Zero-birefringence (ZB) is also desirable as it allows for fewer devices on the test chip, as duplication to satisfy orthogonal polarisations is unnecessary. To date two waveguide profiles have been used to prevent multi-mode behaviour and polarisation dependence. Research is being conducted on two parallel tracks as the conditions cannot be easily satisfied simultaneously. Rib waveguides are good candidates for optical devices as they allow for relatively large waveguide profiles and therefore for a high degree of power usage and lower losses due to fibre-waveguide coupling. Due to their inability to maintain low loss performance for very small radii of curvature (below approximately 10μm), which is crucial for some applications, other solutions started gaining a lot of attention. Strip waveguides, often referred to as silicon wires, have proven to be good candidates with this respect but they are, on the other hand, highly polarisation sensitive.

To consider the design of rib waveguides in more detail, we have simulated the variation of three different values of guiding heights (H), of 1.0μm, 1.35μm, and 1.5μm. By evaluating the TE and TM propagation constants for a series of waveguide widths and etch depths, the ZB locus can be determined for each guiding layer height. The process is one in which we gradually increase the waveguide width until a second-order mode is guided (figure 1). The boundary of the single/multimode can therefore be determined by computing the minimum waveguide width at which the first higher-order mode is supported by the waveguide structure.

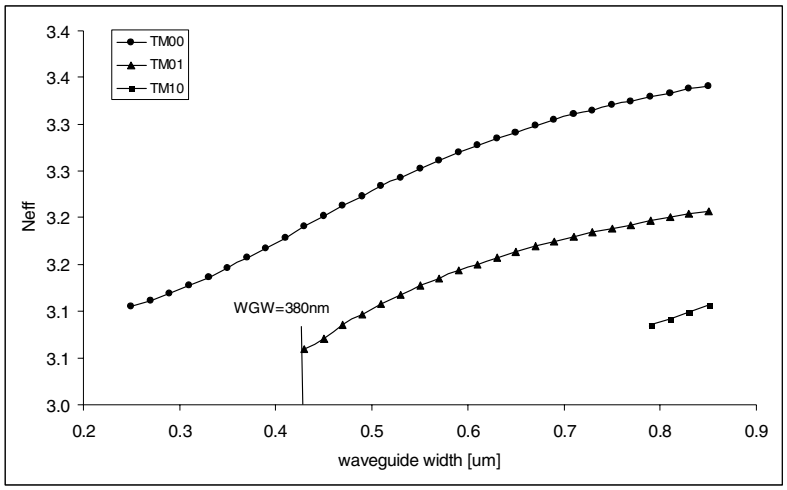

Figure 1. Effective index of the fundamental and the first two higher order TM modes as a function of waveguide width for the rib waveguide with height of H=1.35μm, and etch depth of ED=0.9μm

We have also determined the difference between the effective indices of the fundamental mode as a function of waveguide width and etch depth (ED) for a given waveguide height. The

condition when the effective indices are equal is defined as the zero birefringence condition, and there are up to two such events for each waveguide etch depth (figure 2). By determining these conditions we can plot a "zero birefringence locus" for each waveguide height. By overlapping single-mode and zero-birefringence graphs we can then locate points where ribs are both single-mode and polarisation-birefringent [1].

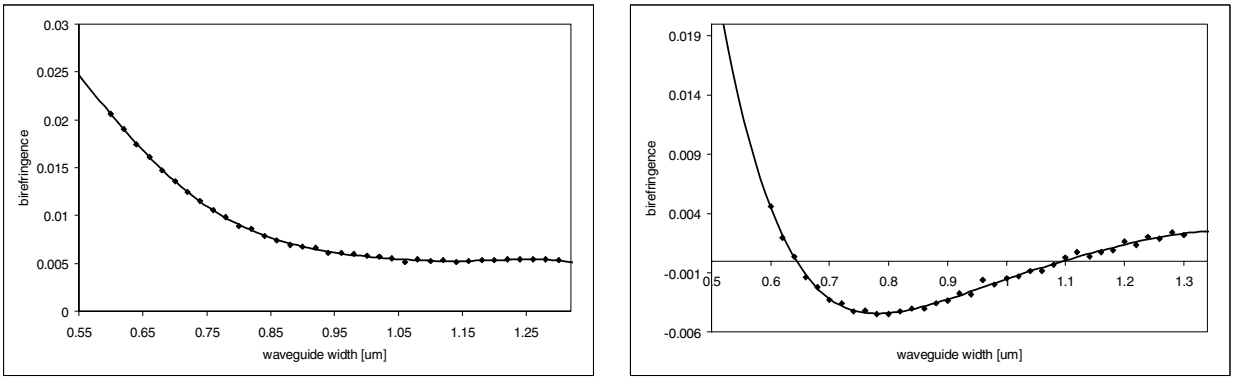

Figure 2. Birefringence in two cases when H=1.35µm: (left) ED=0.675µm, waveguide cannot be polarisation independent, and (right) ED=0.85µm, waveguide ZBR around 0.65µm and 1.1µm

Similar analysis was performed for strip waveguides. The first step in designing strip waveguides for ring resonator filters is to establish single mode (SM) /multimode (MM) boundary. Although 2D simulations are not as accurate as simulations in 3D space, they can give useful guidelines. For instance, we expect that the SM/MM boundary, as predicted by 2D simulations, is slightly relaxed in favour of bigger cross section dimensions for the SM regime, as some apparent higher order modes may be very lossy, or leak out of the structure after several hundred microns of propagation, leaving only the fundamental mode in the structure. The result was obtained by performing 2D simulations for strip waveguides with refractive indices of 3.4764 and 1.444 for the guiding structure and surrounding oxide respectively. It should be noted that it is the TM mode which is critical for waveguide operation in the SM regime. The line representing the boundary between single-mode and multi-mode area can be approximated by the line described by the analytical expression:

$$WGW \leq -1.405 * WGH + 0.746 \quad [\mu m] \tag{1}$$

where WGW and WGH are width and height of the strip waveguide. As an example, in order to prevent propagation of higher order modes, a 0.3µm high waveguide should not be wider than ~0.36µm. Clearly such a restriction has implications for fabrication in terms of resolution, which is why some authors suggest that aiming for polarisation independence in strip waveguides is impractical.

OPTICAL MODULATORS IN SOI

In the design of an optical modulator, four factors are of major importance, the waveguide size, the bandwidth, the efficiency ($L_\pi \cdot V_\pi$) and polarisation independence. The use of depletion modulators using a pn junction is one answer to the bandwidth requirement in silicon photonics as the speed is not limited by the minority carrier lifetime. The drawback of such a technology is

that the length required to achieve a π phase shift in a rib waveguide is in the order of millimetres [2]. In order to improve the real estate of depletion modulators on an optical chip, the efficiency of these devices needs to be improved. The solution could be to use smaller waveguide size as proposed in [2], where the confinement of the mode in a submicron waveguide increase the efficiency of the modulator. The issue with submicron waveguides is the need for efficient optical coupling for TE and TM polarisation [3], as well as losses in the waveguide due to surface roughness and fabrication tolerances. In this paper, we try to provide a solution to the remaining issues, by inserting a pn junction in a micrometer size waveguide which was demonstrated to be polarisation independent in [4]. The proposed modulator is a pn junction formed by a V-shape structure, as shown in figure 3. This structure in figure 1will be compared to a more common structure were a flat pn junction is used as shown in figure 4.

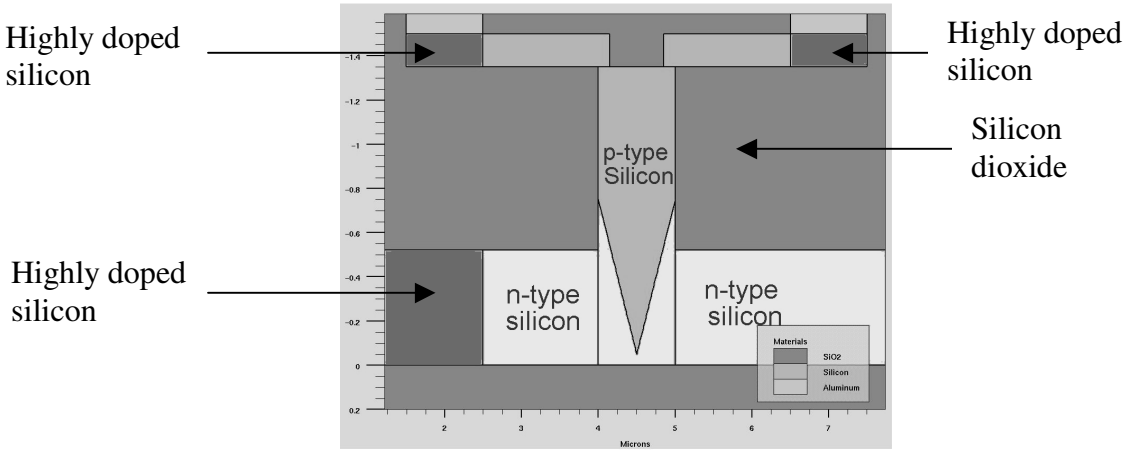

Figure 3. V-shape pn junction optical modulator in silicon technology

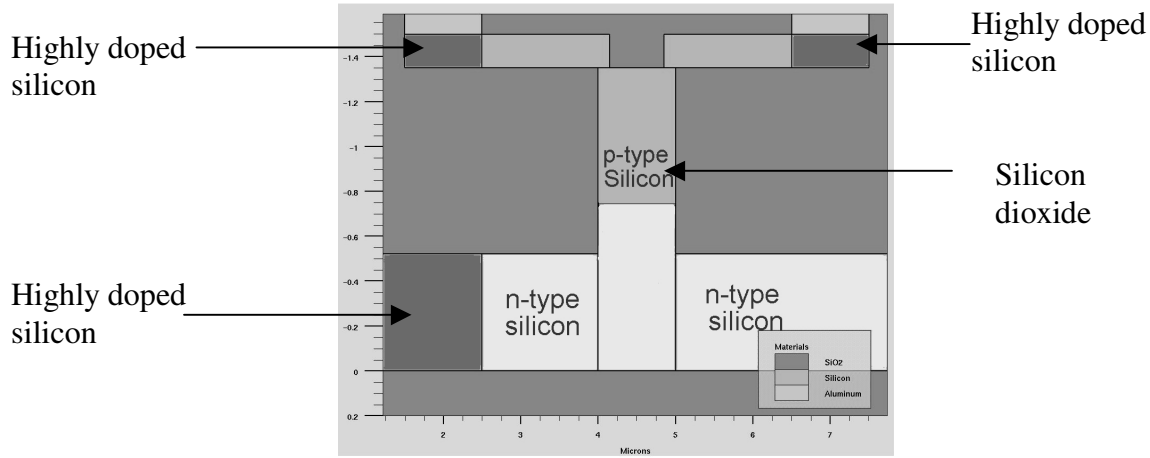

Figure 4. Flat-shape pn junction optical modulator in silicon technology

Optical modelling

The devices were optically modelled using a fully vectorial mode solver. The simulator has been used with full vectorial capability in order to characterise the birefringence-free, single mode waveguide. The active modulator is then introduced to the model. By fitting the change in

refractive index provided by the simulation of the carrier distribution in the devices into the mode solver, it has been possible to predict the effective index change of the waveguides for different voltages, hence calculating the optimum length in order to achieve a π phase shift (equation (2)). The same method has been used to characterise the transient behaviour. The carrier concentration changes at any given bias are introduced into the mode solver for different transient times, hence giving a dynamic change in effective index. Thus using equation 2, the phase shift induced with time can be evaluated.

Electrical modelling

The devices were modelled for both their static and dynamic behaviour using Atlas the device simulation package from Silvaco. Atlas device simulation framework predicts the electrical behaviour of semiconductor devices. It provides a physics-based platform to analyse DC and time domain responses for semiconductor based technologies, by solving the equations which describe semiconductor physics such as Poisson's equation and the charge continuity equations for holes and electrons. The simulator has been used to predict the free carrier concentrations in the waveguiding region of the devices for both DC and transient biasing conditions. The change in the free carrier profile is then converted to refractive index profile in the device using the expressions given by Soref and Bennett equation (2) and equation (3) of [5]. To determine the voltage associated with a π-phase shift, the change in concentration of free carriers must be known. Assuming a non uniform change in refractive index, the active device length required to produce the refractive index change associated with a π-phase shift is obtained approximately from the change in effective index:

$$\Delta n_{eff} = \frac{\lambda}{2L_{\pi}} \tag{2}$$

where λ is the operating wavelength, L_{π} is the active length of the modulator and Δn_{eff} is the change in effective index induced by the change in refractive index Δn in the waveguide. At the wavelength of 1.55μm, which is also the operating wavelength for all simulations here, the refractive index change Δn is given by [5]

$$\Delta n = \Delta n_e + \Delta n_h = -[8.8\times10^{-22}\times\Delta N_e + 8.5\times10^{-22}\times\Delta N_h^{0.8}], \tag{3}$$

where Δn_e is the change in refractive index resulting from the change in free electron concentration, Δn_h is the change in refractive index resulting from the change in free hole concentration, ΔN_e is the change in free electron concentration and ΔN_h is the change in free hole concentration. The following parameters have been used in order to perform the Silvaco simulations.

Table I. Electrical simulation parameters

Surfaces of the waveguides are passivated with SiO_2	
Hole carrier lifetime	300ns
Electron carrier lifetime	700ns
Si background carrier concentration	1×10^{15} ions/cm3
P-type silicon	1×10^{18} ions/cm3
N-type silicon	1×10^{18} ions/cm3
Resistive contact P^+ and N^+	1×10^{19} ions/cm3

Simulation results

The two modulators are based on a polarisation independent, single mode rib waveguide published in [4], and described briefly above. The dimensions are: height H=1.35µm, width W=1µm, and etch depth ED=0.52µm. Both modulators use the depletion of a pn junction in order to change the effective index of the mode propagating in the waveguide. The main difference between the modulators is the shape of the pn junction. Figure 1 show the proposed polarisation independent V-shaped junction, this is created with an angle of 54.7 degrees which is the natural etch angle of silicon. Figure 2 shows a flat pn junction across the waveguide. As the two waveguides are approaching polarisation independence due to their design structure the aim is to show the differences in the phase shift for TE and TM polarisation between both designs while applying a reverse bias.

Efficiency of the modulator and positioning of the junction inside the waveguide

The simulations undertaken below are to determine the polarisation independence of the waveguide during modulation. Figure 5 and 6 show the phase shift achieved for different junction depths and voltages. Figure 5 shows the simulation resulting from the V-shape junction and figure 6 shows similar results for the flat junction. In order to achieve polarisation independence during modulation the optimal positioning of the junction inside the waveguide has to be determined. Figure 5 and 6 show, for both type of junction, the depth where the polarisation independence is achieved. For the v-shaped junction the polarisation independence during modulation is achieved when the top base of the junction is situated around 0.87µm. The flat junction modulator achieves polarisation independence with a junction situated at 0.5µm from the bottom of the waveguide. This is situated at the rib/slab interface which can facilitate easier fabrication.

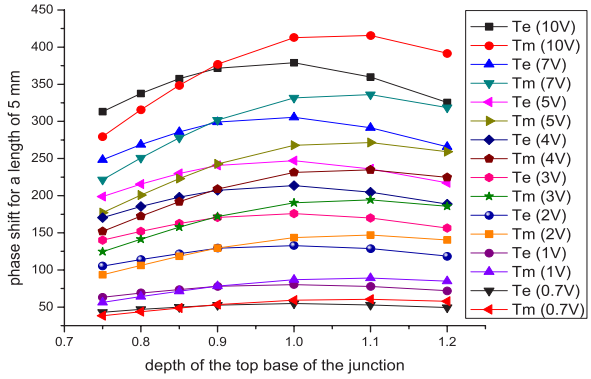

Figure 5. Phase shift modulation dependence for TE and TM using a V-shaped pn junction

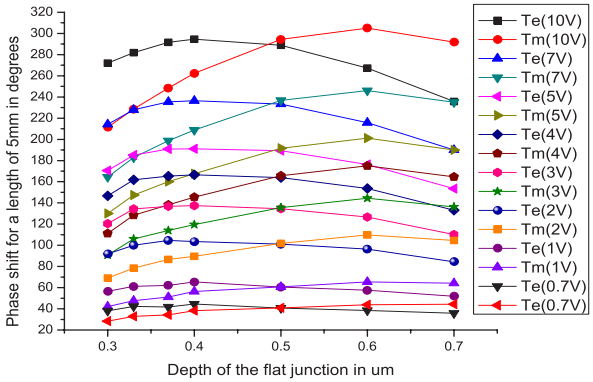

Figure 6. Phase shift modulation dependence for TE and TM using a flat pn junction

The second parameter to extract from those simulations is that the maximum phase shift achieved at polarisation independence for both modulators is different. For a waveguide length of 5mm the V-shaped junction achieve a phase shift of 365 degrees ($L_\pi \cdot V_\pi = 2.5$ V·cm) whereas for the flat junction the maximum phase shift is 290 degrees (($L_\pi \cdot V_\pi = 3.1$ V·cm). These results show that the V-shaped pn junction can achieve the same efficiency as the modulator proposed

in [2] without the problems involved with submicron waveguides. The next step is to determine the bandwidth of both modulators. This is done by calculating the phase shift against transient time and is shown in figures 7 and 8 for TE and TM polarization and for the V junction and flat junction.

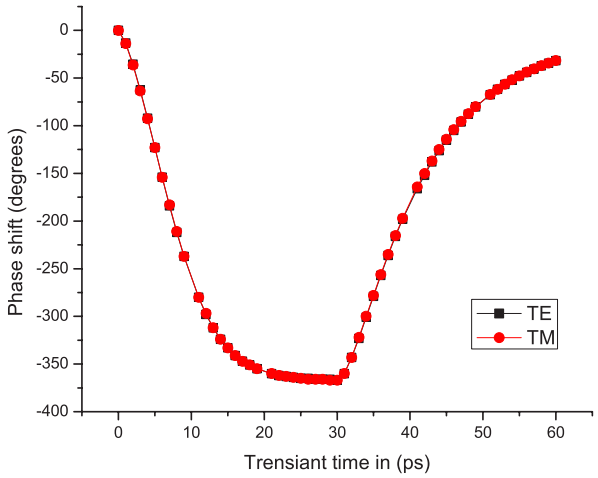

Figure 7. Phase shift against transient time for TE and TM for the V-shaped junction

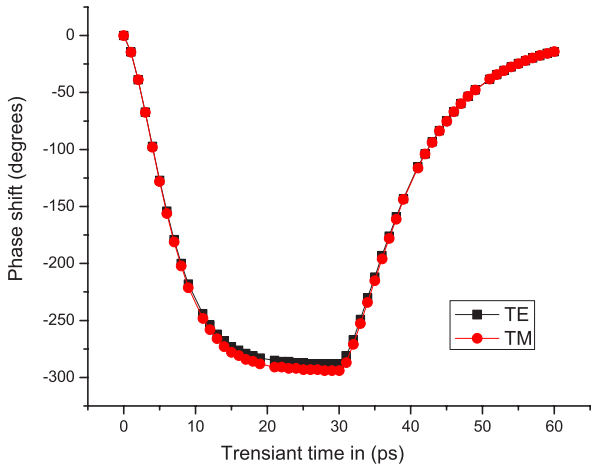

Figure 8. Phase shift against transient time for TE and TM for the flat junction

The transients show that the rise and fall time are similar for both types of junction. For this type of doping, the V-shape junction has a rise time of 13ps and a fall time of 23ps for both TE and TM polarisation. For the flat junction the rise time is 12ps and the fall time is 21ps for both TE and TM. In both cases, this corresponds to an intrinsic bandwidth in excess of 25GHz.

CHARACTERISTICS OF RING AND RACETRACKS RESONATORS

Using the polarisation waveguide design above to design a waveguide coupler, the next step is to address synthesis of photonic devices. Factors such as size and shape of the device, separation between waveguides and their length, concentration of donors and profile of doping region etc can to certain extent also alter response of the device. Passive blocks such as directional coupler and ring resonators are useful elements of various applications (multiplexers for instance) and quite often important part of active blocks (modulators) so it is worth mentioning their design at this stage. The design is once more focused on designing single-mode and polarisation-independent elements but this time with particular care of the spectral response. For majority of photonic devices it is crucial to provide required values for Free Spectral Range (FSR), Full Width at Half Maximum (FWHM) and Quality factor (Q). Commercial applications, for example, impose condition on FSR to be greater than 30nm in optical filters.

Rib and strip directional couplers

Directional couplers are mandatory elements in all resonator structures. Their basic role is to provide efficient transition of the modes from one part of the devices to the other end. They are not likely to significantly change modal properties but polarisation response is typically non-

uniform. This is due to different coupling conditions for TE and TM modes. This means that even utilising ZB waveguides will result in a polarisation dependent coupler.

We can use the results of the previous sections to consider the polarisation properties of strip waveguides. Several different waveguide widths (WGW) were used to investigate polarisation issues of a directional coupler at fixed waveguide height (WGH) of 0.34μm, satisfying the condition given by equation (1), by using the 3D beam propagation method (BPM) and Finite Difference Time Domain (FDTD) analysis. The main purpose of a directional coupler is to allow the propagating wave to transfer from one waveguide to another closely placed straight waveguide or, from the input straight waveguide to the resonator and from the resonator to the output waveguide. The length of the coupler necessary for a mode to be completely transferred is often referred to as the coupling length (CL) of the coupler, which will typically be different for the TE/TM modes. From the polarisation point of view, the directional coupler is a particularly important section of the device as the mode transfer happens in a different fashion for the two modes. Therefore, polarisation independence of the filter directly implies polarisation independence of the directional coupler, which, in turn, sets condition that the coupling lengths corresponding to the TE and TM modes have to be identical. The main goal is therefore to equalise the CLs of the modes by varying parameters such as separation between the waveguides and cross-sectional dimensions.

The values for the CL calculated from simulations for waveguide separation (SEP) of 0.15μm for a fixed waveguide height of 0.34μm and refraction indices of 3.4757 and 1.444 for the guiding structure and the oxide respectively, are plotted in figure 9. From the figure it is possible to identify a WGW at which $CL_{TE} \approx CL_{TM}$. Modelling has not shown a particular tendency in behaviour for other simulated separations ranging from 0.12μm to 0.24μm, but polarisation independence has always been found at a waveguide width located between 0.30μm and 0.45μm. In comparison with the results for SM operation given above, this represents promising result as it predicts the possibility of designing SM and PI small strip resonator filters simultaneously.

In case of rib waveguides we have already demonstrated a way in which SM and ZB conditions can be achieved. By using multiple transitions of TE and TM modes, the length of the coupler can be adjusted to allow the same odd number of transitions for both modes. More precisely, the modelling suggests the use of rib directional couplers with following parameters: waveguide height 1.35μm, waveguide width 0.8μm, length of the coupler 310μm, separation in the coupler 0.5μm or, alternatively, waveguide height 1.35μm, waveguide width 1.0μm, length of the coupler 500μm (1030μm) and separation in the coupler 0.4μm (0.58μm).

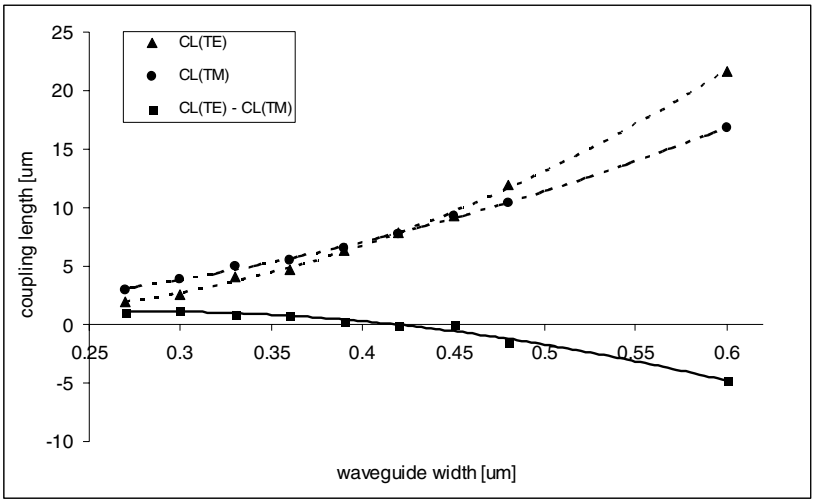

Figure 9. The coupling length as a function of a waveguide width when Sep=0.15μm, WGH=0.34μm, λ=1.55μm

Single ring resonators

The versatility of small resonators put them at the leading edge of potential wavelength selective devices for integrated optics circuits. The filtering feature of the device lies in the fact that only particular resonant harmonics are redirected to specific output ports. By altering the shape of the waveguides and the resonator and its separation from the adjacent straight waveguides, it is possible to change the distance between subsequent resonances and, also, to reshape the pass/stop bands or, in other words, to tune the filter transfer function to the desired response. Since the Free Spectral Range (FSR) is inversely proportional to the resonator circumference [6] the resonator has to utilise bend radii below approximately 5μm if an FSR larger than 30nm is to be achieved. In turn this implies sub-micron dimensions for the waveguide cross sectional dimensions, if such small bend radii are to be sustained. The need for submicron dimensions of a resonator inevitably turned attention to strip waveguides as the main building blocks since they allow the use of the bend radii as small as several microns. As an example, racetracks resonators upon strip waveguides as small as 30nm in circumference give an FSR up to 20nm, whilst very small rings can increase this value above 40nm (figure 10).

This value of FSR would be enough for many applications but the polarisation discrepancy remains a big issue for strip waveguide based devices. The result at the drop port in figure 11 shows that the TE and TM modes can be shifted with respect to one another by several nanometres in the case of small devices. Careful design may correct the shift to certain extent but devices in general show a big tendency towards polarisation dependency. Further investigation and re-design is one possible solution but many researchers see solutions in employing multi-stage configurations.

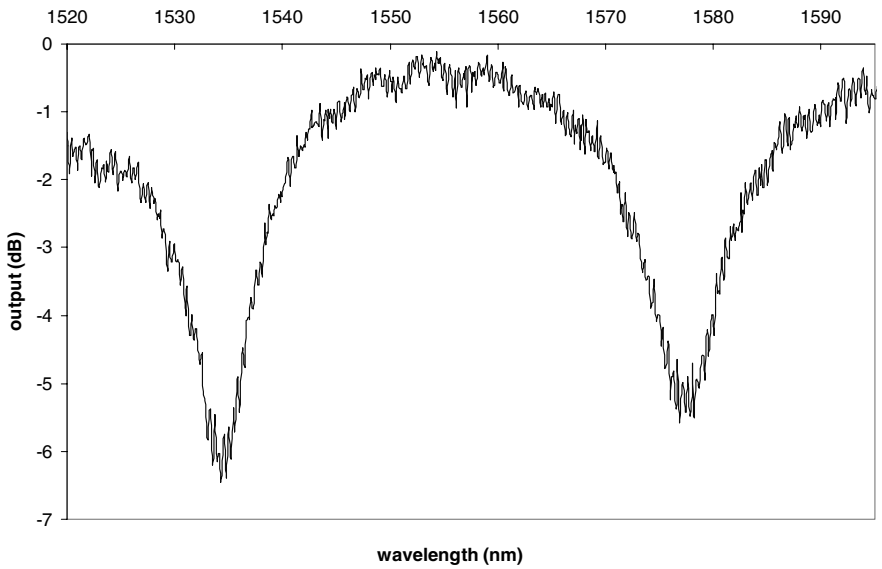

Figure 10. Response of a racetrack resonator, for TM polarisation, with a circumference of 12.57μm, resulting in a free spectral range of 43nm

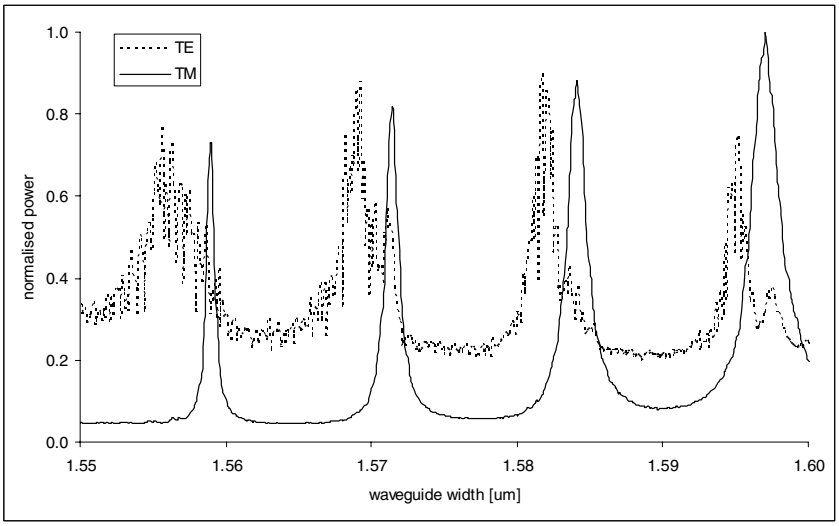

Figure 11. The experimentally obtained transfer function at the drop port of a single racetrack resonator with parameters: WGW=0.34μm, WGH=0.3μm, SEP~0.12μm and length of the coupler = 5.5μm

Tailoring the response by multi-stage resonators

Further improvements of the FSR by decreasing the ring radius below 2μm come at the expense of higher losses and polarisation sensitivity. Alternative solutions in this case could be the implementation of multi-stage parallel-coupled and serial-coupled resonators of larger radius. The resonant condition that has to be satisfied is given by:

$$FSR_{net} = m \times FSR_1 = n \times FSR_2, \quad (4)$$

where m and n are integers, FSR_1 and FSR_2 are free spectral ranges of the two resonators, and FSR_{net} is the net free spectral range of the two-level series coupled resonator.

Modelling has shown that even with relatively large rib resonators improvement can be significant. From several hundreds picometers, the FSR can be increased to several nanometres. For example, by multiplying the experimental responses for 25µm and 50µm one can obtain a prediction for the FSR of cascaded rings, of approximately 2nm (figure 12). Furthermore, such a value can be obtained even with larger resonators provided the resonant condition (4) is met. This point is demonstrated by the graph in figure 13, which is experimentally obtained spectra for cascaded 100µm and 50µm. Despite being promising, this result also show how the output can be sensitive if (4) is not fully satisfied, by exhibiting moderately strong side peaks.

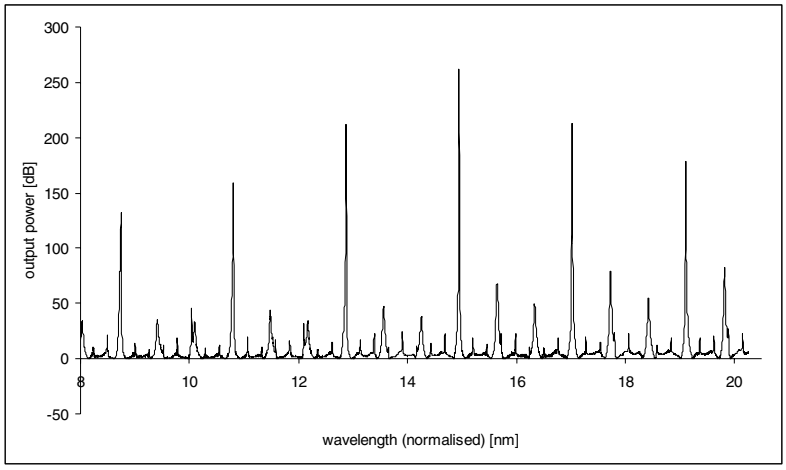

Figure 12. 25µm x 50µm rib racetracks – "modelling"

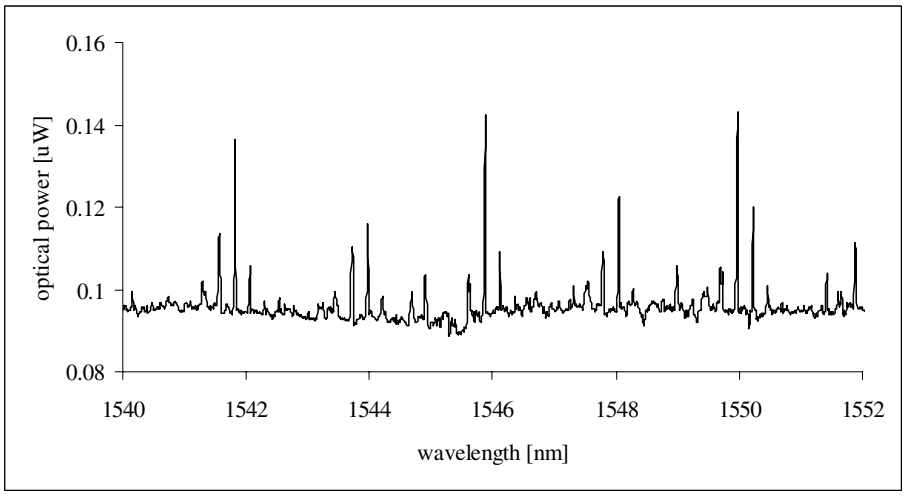

Figure 13. 100µm x 50µm rib racetracks – experiment

CONCLUSIONS

The desire to miniaturise silicon photonic devices for reasons primarily driven by cost and modulation bandwidth can result in these devices being very polarisation dependent. We have

demonstrated that by employing rib waveguides of the order of 1 μm in cross sectional dimensions, optical modulators can still be very fast (bandwidth > 25GHz), but can also exhibit polarization independent performance. Similarly, ring resonators based upon waveguides of the same dimensions can also be polarization independent. Ring resonators based upon smaller rib waveguides are much more difficult to fabricate to be polarization independent, due to both differential phase performance and differential loss, although a large FRS is much easier to obtain that in larger waveguides. Experimental results have been produced to demonstrate these issues with regard to ring resonators, although polarisation independent optical modulators have yet to be realized.

ACKNOWLEDGMENTS

We would like to thank EPSRC, UK, ORSAS, UK, and Intel Corp, USA, for financial support and device fabrication.

REFERENCES

1. S. P. Chan, C. E. Png, S. T. Lim, V. M. N. Passaro, and G. T. Reed, “Single mode and polarisation independent SOI waveguides with small cross section,” *J. Lightwave Technol.*, vol. 23, pp. 1573-1582, 2005.
2. F. Y. Gardes, G. T. Reed, N. G. Emerson, and C. E. Png, "A sub-micron depletion-type photonic modulator in silicon on insulator," *Opt. Express*, vol. 13, pp. 8845-8854, 2005.
3. G. Z. Masanovic, V. M. N. Passaro, and G. T. Reed, "Coupling to nanophotonic waveguides using a dual grating-assisted directional coupler," *IEE Proc. Optoelectronics*, vol. 152, pp. 41-48, 2005.
4. W. R. Headley, G. T. Reed, S. Howe, A. Liu, and M. Paniccia, "Polarisation-independent optical racetrack resonators using rib waveguides on silicon-on-insulator," *Appl. Phys. Lett.*, vol. 85, pp. 5523-5, 2004.
5. R. A. Soref and B. R. Bennett, "Kramers-Kronig analysis of electro-optical switching in silicon," *Proc. SPIE: Integrated Optical Circuit Engineering IV*, 16-17 Sept. 1986, Cambridge, MA, USA, 1987, pp. 32-37.
6. G. Barbarossa, A. M. Matteo, and M. N. Armenise, "Theoretical Analysis of Triple-Coupler Ring-Based Optical Guided-Wave Resonator," *J. Lightwave Technol.*, vol. 13, pp. 148-57, 1995.